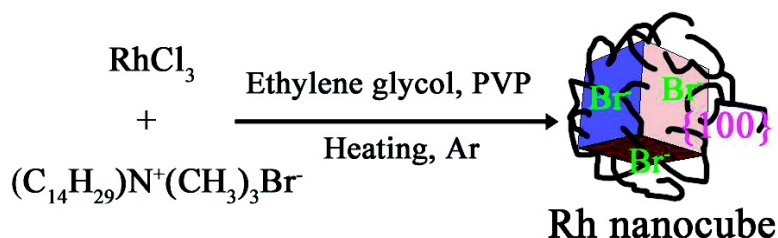


Highly Selective Synthesis of Catalytically Active Monodisperse Rhodium Nanocubes

Yawen Zhang, Michael E. Grass, John N. Kuhn, Feng Tao, Susan E. Habas, Wenyu Huang, Peidong Yang, and Gabor A. Somorjai

J. Am. Chem. Soc., **2008**, 130 (18), 5868-5869 • DOI: 10.1021/ja801210s • Publication Date (Web): 10 April 2008

Downloaded from <http://pubs.acs.org> on February 8, 2009



More About This Article

Additional resources and features associated with this article are available within the HTML version:

- Supporting Information
- Links to the 2 articles that cite this article, as of the time of this article download
- Access to high resolution figures
- Links to articles and content related to this article
- Copyright permission to reproduce figures and/or text from this article

[View the Full Text HTML](#)

Highly Selective Synthesis of Catalytically Active Monodisperse Rhodium Nanocubes

Yawen Zhang,[‡] Michael E. Grass,[‡] John N. Kuhn,[‡] Feng Tao,[‡] Susan E. Habas,[‡] Wenyu Huang,[‡] Peidong Yang,[‡] and Gabor A. Somorjai^{*†}

Department of Chemistry, University of California, Berkeley, California 94720, and the Chemical and Materials Sciences Divisions, Lawrence Berkeley National Laboratory, 1 Cyclotron Road, Berkeley, California 94720, and College of Chemistry and Molecular Engineering, Peking University, Beijing 100871, China

Received February 21, 2008; E-mail: somorjai@berkeley.edu

Synthesis of monodisperse and shape-controlled colloidal inorganic nanocrystals (NCs) is of increasing scientific interest and technological significance.^{1–8} Recently, shape control of Pt,^{1a,3} Pd,⁴ Ag,⁵ Au,⁶ and Rh⁷ NCs has been obtained by tuning growth kinetics in various solution-phase approaches, including modified polyol methods,^{1a,3a,b,4,5a,6a,7a} seeded growth by polyol reduction,^{7b,c} thermolysis of organometallics,^{7d} and micelle techniques.^{3c,5b,6b} Control of noble metal precursors reduction kinetics and regulation of low-index planes (i.e., {100} and {111}) growth rates via selective adsorption are two keys for achieving noble metal NCs shape control. An application for noble metal NCs of well-defined shape is in understanding how NC faceting (determines which crystallographic planes are exposed) affects catalytic performance.²

Rh NCs are used in many catalytic reactions, including hydrogenation,^{8a} hydroformylation,^{8b} hydrocaronylation,^{8c} and combustion reactions.^{8d} Shape manipulation of Rh NCs may be important in understanding how faceting on the nanoscale affects catalytic properties, but such control is challenging and there are fewer reports on the shape control of Rh NCs compared to other noble metals. Xia and co-workers obtained Rh multipods exhibiting interesting surface plasmonic properties by a polyol approach.^{7a} The Somorjai and Tilley groups synthesized crystalline Rh multipods, cubes, horns, and cuboctahedra, via polyol seeded growth.^{7b,c} Son and colleagues prepared catalytically active monodisperse oleylamine-capped tetrahedral Rh NCs for the hydrogenation of arenes via an organometallic route.^{7d} More recently, the Somorjai group synthesized size-tunable monodisperse Rh NCs using a one-step polyol technique.⁹

In this Communication, we report the highly selective synthesis of catalytically active, monodisperse Rh nanocubes smaller than 10 nm by a seedless polyol method. In this approach, Br[−] ions from trimethyl(tetradecyl)ammonium bromide (TTAB) effectively stabilize the {100} faces of Rh NCs and induce the evolution of nanocubes (Scheme 1).

For a typical synthesis, 0.2 mmol RhCl₃ hydrate, 1 mmol TTAB, and 4 mmol poly(vinylpyrrolidone) (PVP, *M*_w = 24 000) were added to 20 mL of ethylene glycol at room temperature. The stock solution was heated to 80 °C and degassed for 20 min under vacuum while stirring, producing a dark brown solution. The flask was then heated to 185 °C and maintained at this temperature for 1.5 h under an Ar atmosphere. When the reaction was complete, an excess of acetone was added to the solution at room temperature to precipitate the nanocubes. The Rh nanocubes were separated

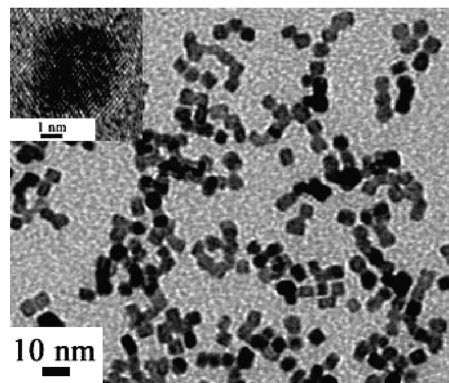
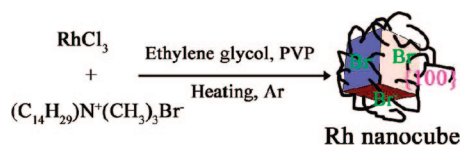


Figure 1. TEM and HRTEM (inset) images of as-obtained Rh nanocubes.

by centrifugation and washed twice by precipitation/dissolution with ethanol/hexanes.

Transmission electron microscopy (TEM, Philips FEI Tecnai 12, 100 kV) revealed the formation of 6.4 ± 0.5 nm (diagonal) Rh nanocubes with >85% selectivity (Figures 1, 2a, and S1a). High resolution TEM (HRTEM, Philips CM200/FEG, 200 kV) (Figure 1 inset) indicated that the Rh nanocubes are single crystalline, enclosed by six {100} faces. Energy dispersive X-ray (EDX) analysis of large areas of the TEM grid suggested that a significant fraction of the Br species was not removed by the precipitation/dissolution steps (Br/Rh = 0.41), and no Cl species were detected (Figure S2). In addition, the EDX spectrum of a single Rh nanocube showed that a small fraction of Br species were associated with the nanocube, suggesting that TTAB should interact with the nanocube surfaces along with the PVP. X-ray diffraction (XRD, Bruker D8 GADDS, Co K α radiation of $\lambda = 1.79$ Å) confirmed the formation of face-centered cubic (*fcc*) Rh (Figure S3). The calculated lattice parameter was $a = 0.3805$ nm for the Rh nanocubes (JCPDS: 0–685). The ratio of $I_{(111)}/I_{(200)}$ obtained for the Rh nanocubes is 2.44, considerably lower than that (3.62–12.5) of Rh polygons of (111) orientation.⁹ X-ray photoelectron spectroscopy (XPS, Perkin-Elmer PHI 5300) demonstrated that the Rh NCs were composed of ~76 atom % Rh(0) and ~24 atom % Rh³⁺ (Figure S4). The intense C 1s and O 1s peaks and the weak N 1s peak, together with the barely detectable Br 3d peak, revealed that

Scheme 1. Seedless Polyol Synthesis of Rh Nanocubes



[‡] University of California, Berkeley, and Lawrence Berkeley National Laboratory.

^{*} Peking University.

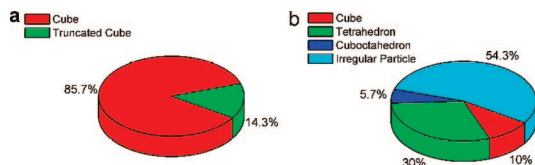


Figure 2. Shape distributions of Rh nanocrystals synthesized in the (a) presence and the (b) absence of TTAB.

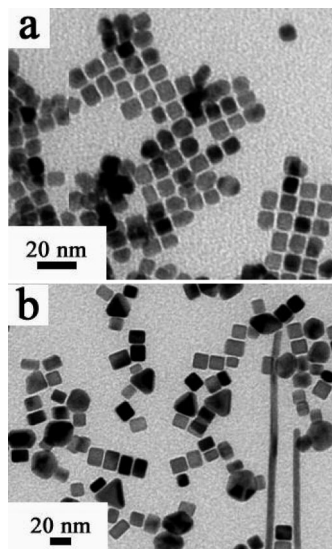


Figure 3. TEM images of as-obtained (a) Pt and (b) Pd nanocubes.

PVP molecules were more strongly adsorbed to the Rh nanocube surfaces than TTAB molecules after washing treatment (Figure S4).

Condition-dependent experiments were conducted to reveal the formation mechanism of the Rh nanocubes. In the absence of TTAB, the use of RhCl_3 as the precursor produced faceted but polydisperse Rh NCs containing some tetrahedral particles (8.2 ± 1.9 nm; Figures 2b and S5a), while RhBr_3 as the precursor yielded monodisperse, but not well-shaped cube-like NCs (40% cubes) (6.3 ± 0.8 nm; Figure S5b). When a mix of RhCl_3 and RhBr_3 was adopted as the precursor, faceted but polydisperse cube-like NCs (39% cubes) were formed (7.6 ± 0.9 nm; Figure S5c). Using RhCl_3 as the precursor and TTAB as the Br^- source, monodisperse Rh nanocubes with significantly enhanced selectivity (>85% cubes; Figure 2a) and monodispersity were obtained with $\text{Rh}^{3+}/\text{TTAB} = 1:5$ (6.4 ± 0.5 nm; Figure 1). When $\text{Rh}^{3+}/\text{TTAB} = 1:1$, monodisperse Rh NCs dominated by truncated cubes with exposed {100} and {111} faces formed (6.3 ± 0.3 nm; Figure S5d). These results strongly suggested that Br^- ions from TTAB effectively stabilize the {100} faces of Rh, and Br^-/Cl^- pairs regulate the relative growth rate along the <100> and <111> directions.^{4c}

Pt and Pd nanocubes can be also prepared by the same synthetic procedure. Reduction of $(\text{NH}_4)_2\text{PtCl}_6$ ($\text{Pt}^{4+}/\text{TTAB} = 1:15$) at 180 °C for 1 h produced 10.0 ± 0.8 nm Pt nanocubes (74% cubes, 20% cuboctahedra, 6% polyhedra) (Figures 3a and S1b). Reduction of $(\text{NH}_4)_2\text{PdCl}_6$ ($\text{Pd}^{4+}/\text{TTAB} = 1:15$) at 140 °C for 1 h generated 17.4 ± 3.2 nm Pd nanocubes (56% cubes, 23% bars, 1% rods, and 20% polyhedra) (Figures 3b and S1c). The calculated lattice constants were $a = 0.3913$ nm for the Pt nanocubes (JCPDS: 4–802) and $a = 0.3867$ nm for the Pd nanocubes (JCPDS: 46–1043) (Figure S3).

As-synthesized Rh nanocubes were deposited onto silicon wafers by the Langmuir–Blodgett (LB) technique to form two-dimensional nanoarray catalysts,⁹ which were then tested for pyrrole hydrogenation and CO oxidation. For pyrrole hydrogenation, the

Rh catalysts fully hydrogenated pyrrole to *n*-butane and ammonia between 303 and 343 K. The turnover frequency (TOF) did not strongly depend on temperature (Figure S6a). Detailed catalytic results on activity and selectivity will be presented for pyrrole hydrogenation in comparison with a Rh(100) single crystal elsewhere. For CO oxidation, the TOF monotonically increased from 0.74 s^{-1} at 463 K to 12.7 s^{-1} at 503 K (Figure S6b) and was comparable to those reported for a Rh(100) single crystal.¹⁰ The apparent activation energy for CO oxidation was 35 kcal mol^{-1} , higher than that reported ($25.4 \text{ kcal mol}^{-1}$) for the Rh(100) single crystal, possibly due to the adsorption of the capping ligands on the nanocube surfaces.¹⁰

In conclusion, monodisperse sub-10 nm Rh nanocubes were synthesized with high selectivity by a seedless polyol method. The {100} faces of the Rh NCs were effectively stabilized by chemically adsorbed Br^- ions from TTAB. This simple one-step polyol route can be readily applied to the preparation of Pt and Pd nanocubes. Moreover, the organic molecules of PVP and TTAB that encapsulated the Rh nanocubes did not prevent catalytic activity for pyrrole hydrogenation and CO oxidation. We are now investigating the shape-dependent activity and selectivity of the Rh NCs for several heterogeneous reactions.

Acknowledgment. This work was supported by the Director, Office of Science, Office of Basic Energy Sciences, Division of Materials Sciences and Engineering of the U.S. Department of Energy under Contract No. DE-AC02-05CH11231, and portions of this work were performed at the Molecular Foundry, Lawrence Berkeley National Laboratory. Y.W.Z. appreciates the financial aid of Huaxin Distinguished Scholar Award from Peking University Education Foundation of China.

Supporting Information Available: More TEM images, size distribution histograms, XPS and EDX data, catalytic data, and detailed synthetic procedures. This material is available free of charge via the Internet at <http://pubs.acs.org>.

References

- (1) (a) Ahmadi, T. S.; Wang, Z. L.; Green, T. C.; Henglein, A.; El-Sayed, M. A. *Science* **1996**, *272*, 1924. (b) Peng, X.; Manna, L.; Yang, W.; Wickham, J.; Scher, E.; Kadavanich, A.; Alivisatos, A. P. *Nature* **2000**, *404*, 59. (c) Sun, S.; Murray, C. B.; Weller, D.; Folks, L.; Moser, A. *Science* **2000**, *287*, 1989. (d) Yin, Y.; Alivisatos, A. P. *Nature* **2005**, *437*, 664. (e) Narayanaswamy, A.; Xu, H.; Pradhan, N.; Kim, M.; Peng, X. *J. Am. Chem. Soc.* **2006**, *128*, 10310. (f) Habas, S. E.; Lee, H.; Radmilovic, V.; Somorjai, G. A.; Yang, P. *Nat. Mater.* **2007**, *6*, 692.
- (2) (a) Narayanan, R.; El-Sayed, M. A. *J. Phys. Chem. B* **2005**, *109*, 12663. (b) Tian, N.; Zhou, Z. Y.; Sun, S. G.; Ding, Y.; Wang, Z. L. *Science* **2007**, *316*, 732.
- (3) (a) Song, H.; Kim, F.; Connor, S.; Somorjai, G. A.; Yang, P. *J. Phys. Chem. B* **2005**, *109*, 188. (b) Chen, J.; Herricks, T.; Xia, Y. *Angew. Chem., Int. Ed.* **2005**, *44*, 2589. (c) Lee, H.; Habas, S. E.; Kweskin, S.; Butcher, D.; Somorjai, G. A.; Yang, P. *Angew. Chem., Int. Ed.* **2006**, *45*, 7824.
- (4) (a) Xiong, Y.; Chen, J.; Benjamin, J. W.; Xia, Y.; Aloni, S.; Yin, Y. *J. Am. Chem. Soc.* **2005**, *127*, 7332. (b) Xiong, Y.; McLellan, J. M.; Yin, Y.; Xia, Y. *Angew. Chem., Int. Ed.* **2007**, *46*, 790. (c) Xiong, Y.; Cai, H.; Wiley, B. J.; Wang, J.; Kim, M. J.; Xia, Y. *J. Am. Chem. Soc.* **2007**, *129*, 3665.
- (5) (a) Tao, A.; Sinsersuksakul, P.; Yang, P. *Angew. Chem., Int. Ed.* **2006**, *45*, 4597. (b) Chen, S.; Carroll, D. L. *J. Phys. Chem. B* **2004**, *108*, 5500.
- (6) (a) Seo, D.; Park, J. C.; Song, H. *J. Am. Chem. Soc.* **2006**, *128*, 14863. (b) Wu, H.-Y.; Liu, M.; Huang, M. H. *J. Phys. Chem. B* **2006**, *110*, 19291.
- (7) (a) Zettsu, N.; McLellan, J. M.; Wiley, B.; Yin, Y.; Li, Z.-Y.; Xia, Y. *Angew. Chem., Int. Ed.* **2006**, *45*, 1288. (b) Humphrey, S. M.; Grass, M. E.; Habas, S. E.; Niesz, K.; Somorjai, G. A.; Tilley, T. D. *Nano Lett.* **2007**, *7*, 785. (c) Hoefelmeyer, J. D.; Niesz, K.; Somorjai, G. A.; Tilley, T. D. *Nano Lett.* **2005**, *5*, 435. (d) Park, K. H.; Jang, K.; Kim, H. J.; Son, S. U. *Angew. Chem., Int. Ed.* **2007**, *46*, 1152.
- (8) (a) Pellegatta, J.-L.; Blandy, C.; Collière, V.; Choukroun, R.; Chaudret, B.; Cheng, P.; Philippot, K. *J. Mol. Catal. A* **2002**, *178*, 55. (b) Yoon, T.-J.; Kim, J. I.; Lee, J.-K. *Inorg. Chim. Acta* **2003**, *345*, 228. (c) Haltunen, M. E.; Niemelä, M. K.; Krause, A. O. I.; Vaara, T.; Vuori, A. I. *Appl. Catal., A* **2001**, *205*, 37. (d) Gayen, A.; Baidya, T.; Biswas, K.; Roy, S.; Hegde, M. S. *Appl. Catal., A* **2006**, *315*, 135.
- (9) Zhang, Y.; Grass, M. E.; Habas, S. E.; Tao, F.; Zhang, T.; Yang, P.; Somorjai, G. A. *J. Phys. Chem. C* **2007**, *111*, 12243.
- (10) Peden, C. H. F.; Goodman, D. W.; Blair, D. S.; Berlowitz, P. J.; Fisher, G. B.; Oh, S. H. *J. Phys. Chem.* **1988**, *92*, 1563.

JA801210S